

A counter-rotating tilted gas disc in the peanut galaxy NGC 128 ^{*}

Eric Emsellem¹ and Robin Arsenault²

¹ European Southern Observatory, Karl-Schwarzschild Strasse 2, D-85748 Garching b. München, Germany

² Canada-France-Hawaii Corporation, P.O. Box 1597, Kamuela, HI 96743, USA

accepted 07/01, 1996

Abstract. We have obtained V , R_c , I_c HRCAM images and TIGER spectrography of the central region of the peanut galaxy NGC 128. The colour images reveal the presence of a red disc tilted by about 26 degrees with respect to the major-axis of the galaxy. This tilted disc is made of dust and gas, as revealed by the 2D TIGER map of the ionized gas distribution. The TIGER stellar and gas velocity fields show that the angular momentum vectors of the stellar and gaseous components are reversed. We therefore suggest that the gas orbits belong to the so-called anomalous family, which is evidence for a tumbling triaxial potential (a bar) associated with the peanut morphology. The bar formation has very probably been triggered through the interaction with its nearby companion NGC 127, from which the dissipative component is being accreted along retrograde orbits.

Key words: ISM: kinematics and dynamics – galaxies: NGC 128 – galaxies: interactions – galaxies: kinematic and dynamics – galaxies: nuclei

1. Introduction

N body simulations have shown that strong bars can appear as peanut-shaped bulges when viewed close to edge-on (Combes & Sanders 1981, Combes et al. 1990, Pfenniger & Friedli 1991). The same bar would be seen nearly round when end-on and box-shaped for an intermediate viewing angle. These morphologies are indeed observed in galaxies, which suggested that boxy and peanut-like bulges could be linked to the presence of bars. Recently,

Send offprint requests to: E. Emsellem (email: eemselle@eso.org)

^{*} Based on observations taken with the Canada-France-Hawaii Telescope, operated by the National Research Council of Canada, the Centre National de la Recherche Scientifique of France, and the University of Hawaii

Kuijken & Merrifield (1995) have shown that it is possible to detect edge-on bars kinematically by a careful study of the projected velocity distribution. When a tumbling triaxial structure is present, the observed Line Of Sight Velocity Distributions (LOSVDs) should exhibit contrasted gaps corresponding to the transition regions between the main resonances. They indeed detected these expected features in two peanut-shaped galaxies. A larger sample has recently been analysed by Bureau & Freeman (1997) who found the signature of a bar in nearly all systems. This technique is powerful to detect bars in edge-on systems. However it requires the presence of a rather extended gas disc¹. It may therefore be a difficult task to apply this method systematically on all boxy/peanut bulges.

In this Letter, we show that in exceptional circumstances the signature of the bar is even more obvious. This is illustrated with the prototype of peanut-shaped galaxy, namely NGC 128. Although this “peculiar” S0 galaxy appears in the Hubble Atlas, it has been only scarcely studied. Bertola & Capaccioli (1977) published a combined photometric and spectroscopic analysis of NGC 128, including the derivation of its major-axis velocity profile. It was also included in the sample of early-type galaxies observed by Bertola et al. (1992) who obtained long-slit spectrography along the major-axis, and only commented on the mean angular momenta of the stars and gas concluding that they had the same direction. This is, as will be shown in this Letter, inconsistent with our TIGER data (preliminary results published in Monnet et al. 1995; see also Pagan et al. 1996 and Kuijken et al. 1996).

Details on our observations are given in Sect. 2. The corresponding results are presented in Sect. 3. A brief discussion and some conclusions are drawn in Sect. 4.

¹ Since star orbits can “cross” each other, the bar signature is weaker in stellar LOSVDs (see Kuijken & Merrifield 1995).

2. Observations

2.1. Photometry

V , R_c and I_c (Cousin system) images of NGC 128 were obtained with HRCAM at the CFHT in Dec. 1993. These exposures were reduced in the classical way under IRAF. Bad columns present on the CCD were interpolated using the adjacent pixels. We normalized the images using the available aperture photometry (de Vaucouleurs & Longo 1988; Poulain 1986, 1988), leading to an uncertainty of about 0.05 magnitude. All images were then centred and rotated such that the major-axis (for $R < 10''$) of NGC 128 is horizontal (measured PA of 1.9 ± 1 degrees). The resulting spatial resolution is poor and nearly identical for all images: FWHM of $\sim 1''.1$. We computed the $V - R_c$ and $V - I_c$ colour images, which were smoothed through a simple gaussian convolution with $\sigma = 0''.25$.

2.2. Spectroscopy

We also observed NGC 128 in Nov. 1993 using the integral field spectrograph TIGER mounted on the Cassegrain focus of the CFHT. The lens diameter was set to $0''.39$ giving a field of $\sim 7'' \times 7''$. Two spectral domains were covered: one around the Mg triplet (5100–5500 Å) and another including the [N II]/H α and [S II] emission lines (6530–6990 Å) both with a sampling of 1.5 Å/px. The standard reduction steps were applied to extract and calibrate the spectra of each individual exposure, using the TIGER software (Bacon et al. 1994). A total of 3 hours were obtained for the absorption line domain ($\sigma_\star = 0''.47$, $\sigma_{spec} \sim 75 \text{ km.s}^{-1}$; hereafter “blue spectra”) and 2.5 hours for the emission lines ($\sigma_\star = 0''.42$, $\sigma_{spec} \sim 60 \text{ km.s}^{-1}$; hereafter “red spectra”)

The stellar kinematics were derived from the blue spectra using the FCQ method of Bender (1990) which provides the full LOSVD for each spatial element. We will however only report here the estimates of the two first moments derived from a gaussian fit: at our spectral (and spatial) resolution the derived LOSVDs in the central part of NGC 128 do not deviate significantly from single Gaussians.

The red spectra of NGC 128 exhibit the H α , [N II] and [S II] emission lines, all detected in the central part of NGC 128. In order to obtain pure emission line spectra, we first had to subtract the stellar continuum from the original spectra. We thus used a high resolution spectrum of the emission-line free elliptical NGC 596 kindly provided by Paul Goudfrooij. The relative doppler shift ΔV and broadening $\Delta\sigma$ of the blue part of NGC 596’s spectrum with respect to the TIGER blue spectra of NGC 128 were determined using FCQ. The broadened spectrum of NGC 596 was then scaled to each individual TIGER red spectrum of NGC 128 and subtracted. Low frequency differences between the stellar continua of NGC 596 and NGC 128 were included using a low-order polynomial. The

resulting pure emission line spectra were analysed with the FITSPEC software written by A. Rousset (Lyon Observatory).

3. Results

3.1. The morphology of NGC 128

As already emphasized in previous studies (e.g. Bertola & Capaccioli 1977), the outer disc of NGC 128 is bending towards its companion NGC 127 (westwards), certainly due to the interaction (Fig. 1). The NGC 128 group contains another small galaxy NGC 130: although the latter probably participates in the interaction (Jarvis 1990), we did not detect any luminous bridge between NGC 128 and NGC 130. The peanut in NGC 128 appears as an additional “quadrupole component” whose maxima lie at $x = \pm 10''$ (along the major-axis) and $y = \pm 8''$ (minor-axis). NGC 128 also contains a central thin disc extending up to $\sim 7''$.

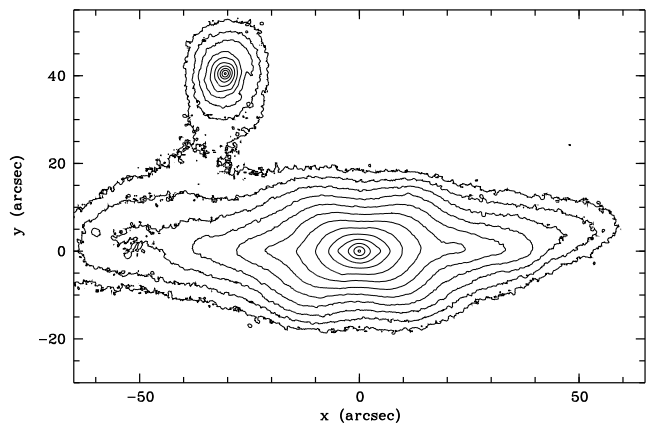


Fig. 1. HRCAM I_c band image of the prototypical peanut galaxy NGC 128. The step is $0.5 \text{ mag.arcsec}^{-2}$ and the faintest isophote corresponds to $21.5 \text{ mag.arcsec}^{-2}$. The small galaxy in the top left is NGC 127, a small interacting companion. The interaction between the two galaxies is clearly seen here.

3.2. A tilted red disc

In the central $6''$, the $V - R_c$ and $V - I_c$ colour images exhibit flattened isocontours which are tilted by ~ 26 degrees with respect to the major-axis of the galaxy (Fig. 2). The R_c band includes the H α , [N II] and [S II] emission lines which could produce part of this reddening. However, our I_c filter only contains the [SIII] $\lambda 9069$ emission line which should represent less than 10% of the total nebular emission in the R_c filter. The reddening in $V - I_c$ would correspond to a relative extinction of $E(V - I_c) \sim 0.02$. In order to search for the presence of dust we have symmetrized the V band image with respect to the minor-axis: we found

a difference of ~ 0.045 magnitude between the surface brightness along the disc and at its symmetric point. This would be consistent with the $V - I_c$ reddening being entirely due to dust extinction (assuming ‘Galactic dust’, Emsellem 1995). The expected dust reddening $E(V - R_c)$ would then be smaller than 0.01 magnitude.

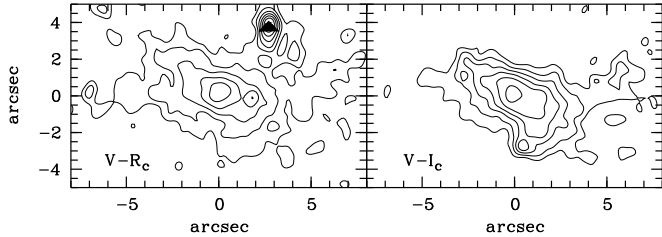


Fig. 2. $V - R_c$ (left) and $V - I_c$ (right) isocolours of the central region of NGC 128: the step is 0.01 magnitude and the maxima are 0.58 and 1.34 respectively for the $V - R_c$ and $V - I_c$ contours. The secondary maximum in the $V - R_c$ plot is due to a CCD defect (black triangle).

3.3. Gas distribution and kinematics

The red spectra exhibit rather narrow emission lines ($85 < \sigma(\text{km.s}^{-1}) < 135$) throughout the TIGER field except in the central arcsecond where a superimposed broad $H\alpha$ component is marginally detected. This component seems to be redshifted with respect to the narrow line system by $\sim 450\text{km.s}^{-1}$, and has a FWHM of $\sim 2590\text{km.s}^{-1}$ (Fig. 3). However, the presence of a Broad Line Region (BLR) should be confirmed with higher signal to noise data.

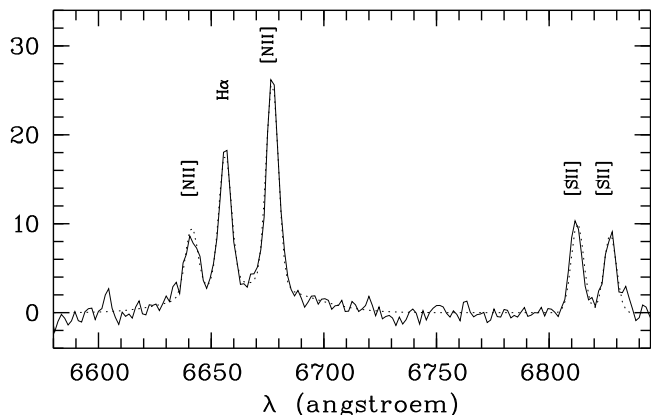


Fig. 3. Sum of the 5 central TIGER spectra (stellar continuum subtracted) showing the $[\text{N II}]$, $H\alpha$, and $[\text{S II}]$ narrow lines as well as the broad $H\alpha$ line. The best fit derived with FITSPEC is superimposed (dotted line).

Fig 4 shows the gas distribution of the $[\text{N II}]\lambda 6583$ emission line: the gas is distributed in a disc-like structure whose major-axis is tilted by ~ 26 degrees with respect to the I_c band major-axis of the core. This is very similar to the central feature detected in the $V - R_c$ image which demonstrates that the gas disc certainly extends at least up to $6''$ ($\sim 1750\text{pc}$ at 60Mpc) from the centre. The $[\text{N II}]\lambda 6583$ to $H\alpha$ ratio slightly rises towards the centre from about 1.2 to 1.65. The ratios $[\text{S II}]/H\alpha$ and $[\text{S II}]\lambda 6717/[\text{S II}]\lambda 6731$ are in the ranges $[0.8 - 1.5]$ and $[0.7 - 1.5]$ respectively, typical for a LINER, and consistent with the gas being photoionized by post-AGB stars (Binette et al. 1994).

The TIGER gas velocity field beautifully confirms the tilt of the gas disc: the zero isovelocity (w.r.t. the systemic velocity of the galaxy) is tilted by ~ 25 degrees consistent with the position angle of the gas distribution minor-axis. Since dust is associated with the gaseous component, we rejected the hypothesis of a linear ejection from the centre. At our resolution, the gas thus exhibits nearly cylindrical rotation with $\Omega \sim 67\text{km.s}^{-1}.\text{arcsec}^{-1}$.

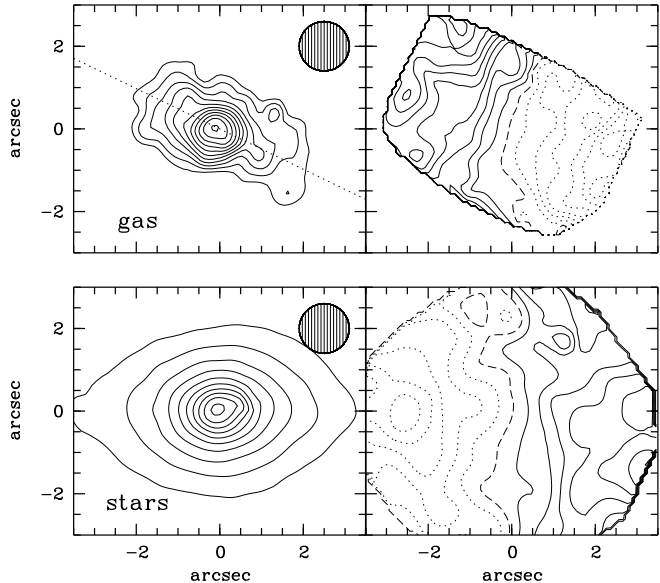


Fig. 4. 2D distributions (left panels) and velocity fields (right panels) of the gas ($[\text{N II}]\lambda 6583$ line, top) and stellar (bottom) components. The dotted straight line in the top left panel shows the gas mean major-axis at 26 degrees. The isovelocity step is 25km.s^{-1} in both cases (the dotted lines correspond to negative velocities, the solid lines to positive). The gas maps have been smoothed by a gaussian with $\sigma = 0''.3$. The drawn beams correspond to the seeing FWHMs in each configuration.

3.4. Stellar kinematics

The picture gets even more striking when we compare the velocity fields of the stellar and gaseous components

(Fig. 4): their mean angular momenta are reversed. The maximum stellar velocities ($\pm 140 \text{ km.s}^{-1}$) are reached at the edge of our field. The velocity dispersion field exhibits a central dip with $\sigma_0 \sim 205 \text{ km.s}^{-1}$ and shows the presence of a cold component (i.e. the inner disc) along the major-axis.

4. Discussion and conclusions

The regularity of the velocity field of the gas suggests that it has settled onto closed orbits in the centre. In an axisymmetric potential, gas would rapidly fall onto the equatorial plane of the galaxy in a few orbital periods². This process seems to be even more efficient if the potential is triaxial and stationary (Colley & Sparke 1996). However, tumbling triaxial potentials are known to contain stable families of closed orbits which leaves the plane perpendicular to the rotation axis (see e.g. Magnenat 1982, Mulder & Hooimeyer 1984). The main family of retrograde orbits is then the so-called ANomalous Orbits (ANO) which corresponds to the 1:1 vertical resonance. For slow figure rotation Ω_p these orbits bifurcates from the E_z family. Above a certain critical value $\Omega_{p_{crit}}$, the z -orbit become complex unstable. The value of $\Omega_{p_{crit}}$ is significantly lowered as soon as a small central mass concentration is present (see Martinet & Pfenniger 1987, and Pfenniger & Friedli 1991 for further details).

We therefore conclude that the potential of NGC 128 must be triaxial and tumbling. In other words, the prominent peanut in NGC 128 corresponds to a bar viewed nearly edge-on. The maximum of the peanut corresponds to the axisymmetric horizontal and vertical inner Lindblad resonances: $\Omega_p = \Omega - \kappa/2 = \Omega - \nu_z/2$ (Combes et al. 1990). In a forthcoming paper, we will present a realistic mass model of NGC 128 built using the generalization of the Multi-Gaussian Expansion method (Emsellem 1993). Preliminary results from this model indicate that the pattern speed must be high with $\Omega_p > 30 \text{ km.s}^{-1}.\text{kpc}^{-1}$, and therefore suggests that it overcomes the critical boundary $\Omega_{p_{crit}}$. The morphology of the retrograde gas orbits in such a case (“fast Ω_p ”) are nicely illustrated in Fig. 3 of Friedli & Udry (1993): they are circling the long-axis of the bar, and their edge-on projection shows a central tilted disc structure very similar indeed to the one observed in NGC 128. A detailed dynamical model is required to confirm that this interpretation is fully consistent with the observed kinematics.

The peanut itself is not perfectly symmetric and exhibits some distortions: this is certainly the result of the interaction with NGC 127. We suggest that the interaction with the small satellite NGC 127 (whose integrated luminosity in the I_c band is $\sim 7\%$ of NGC 128’s) triggered the formation of a bar in NGC 128 and accelerated its dynamical evolution leading to its peanut-shape. There

is a gap between the two discs along the major-axis which closely corresponds to the location of the maximum of the peanut. This is expected if the stars populating the peanut were driven out of the equatorial plane of the galaxy. This double disc structures intriguingly resembles the ones observed in many S0s (Seifert & Scorza 1996).

The observed ionized gas in NGC 128 has almost certainly an external origin. Our photometric data show that NGC 127 contains a significant amount of dust (see Fig. 1) and therefore very probably some gas. It is however difficult to say whether this has been accreted to form the tilted red disc observed today in NGC 128: it could have been formed during an earlier accretion event. Finally, if NGC 127 is later cannibalized by NGC 128, it is likely that the bar would be destroyed in the process leading to a nearly axisymmetric bulge (Pfenniger 1991).

References

- Bacon, R., Emsellem, E., Monnet, G., Nieto, J.-L., 1994, *A&A*, 281, 691
- Bender, R., 1990, *A&A* 229, 441
- Bertola, F., Capaccioli, M., 1977, *ApJ* 211, 697
- Bertola, F., Buson, L. M., Zeilinger, W. W., 1992, *ApJ* 401, L79
- Binette, L. Magris, C. G., Stasinska, G., Bruzual, A. G., *A&A* 292, 13
- Bureau, M., Freeman, K., 1997. In M. Arnaboldi, G. Da Costa, & P. Saha (eds.) *The Nature of Elliptical Galaxies*, (in press)
- Colley, W. N., Sparke, L., 1996, *ApJ* 471, 748
- Combes, F., Sanders, R. H., 1981, *A&A* 96, 164
- Combes, F., Debbasch, F., Friedli, D., Pfenniger, D., 1990, *A&A* 233, 82
- de Vaucouleurs, A., Longo, G., 1988, Univ. of Texas, Austin
- Emsellem, E., 1993, PhD Thesis, Université Paris VII
- Emsellem, E., 1995, *A&A* 303, 673
- Friedli, D., Udry, S., 1994. In H. Dejonghe & H. Habing (eds.) *Proc. IAU Symp. Galactic Bulges*, Gent, p. 273
- Jarvis, B., 1990. In R. Wielen (ed.) *Dynamics and Interactions of Galaxies*, p. 416
- Kuijken, K., Merrifield, M. R., 1995, *ApJ* 443, L13
- Kuijken, K., Fisher, D., Merrifield, M. R., 1996, *MNRAS* (in press)
- Magnenat, P., *A&A* 108, 89
- Martinet, L., Pfenniger, D., 1987, *A&A* 173, 81
- Monnet, G., Emsellem, E., Pécontal, E., Thiébaud, E., 1995, 5th Tex-Mex Symposium, Mexico
- Mulder, W. A., Hooimeyer, J. R. A., *A&A* 134, 158
- Pagan, A., D’Onofrio, M., Capaccioli, M., Zaggia, S., 1996, In G. Longo et al (eds.) *Interacting Galaxies*, in press.
- Pfenniger, D., 1991. In B. Sundelius (ed.) *Dynamics of disc Galaxies Göteborg*, p. 191
- Pfenniger, D., Friedli, D., 1991, *A&A* 252, 75
- Poulain, P., 1986, *A&AS*, 64, 225
- Poulain, P., 1988, *A&AS*, 72, 215
- Seifert, W., Scorza, C., 1996, *A&A* 310, 75

This article was processed by the author using Springer-Verlag L^AT_EX A&A style file *L-AA* version 3.

² The orbital time is estimated to be $\sim 26 \text{ Myr}$ at $2''$.